



Gamow-Teller excitations in open-shell nuclei at finite temperature

Esra Yüksel

Department of Physics, Faculty of Science, University of Zagreb, Croatia
Department of Physics, Faculty of Science and Letters, Yıldız Technical University, Istanbul, Turkey

Collaborators: Nils Paar, Yifei Niu



Europska unija
Zajedno do fondova EU



Operativni program
KONKURENTNOST
I KOHEZIJA

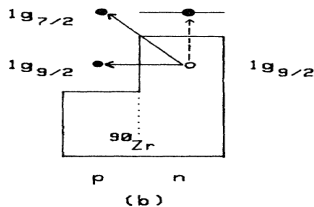
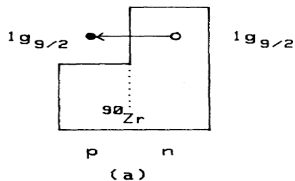
Outline

- 1 Introduction and motivation
 - Spin-isospin excitations in nuclei
- 2 Microscopic models
 - Relativistic finite temperature proton-neutron QRPA
- 3 Numerical results
 - Gamow-Teller excitations at finite temperature
- 4 Conclusions and perspectives
- 5 Acknowledgments

Image by Andy Sproles, Oak Ridge National Laboratory.

Introduction and motivation: spin-isospin excitations

- ✓ The spin-isospin resonances can be induced by isospin lowering (τ_-) or raising (τ_+) operators.
 - Isobaric analog states (IAS):
 $\Delta L = \Delta J = \Delta S = 0$,
 - Gamow-Teller resonance (GTR):
 $\Delta L = 0, \Delta J = \Delta S = 1$,
 - Spin monopole ($J = 0^-$), dipole ($J = 1^-$) and quadrupole ($J = 2^-$) states.
- ✓ Their properties are important to understand the nuclear structure:
 - Spin and isospin properties of the effective nuclear interaction
M. Bender et al., PRC 65, 054322 (2002), H. Liang et al., PRL 101 (2008) 122502.,
 - They can be used to predict neutron skin thickness of nuclei
D. Vretenar et al., Phys.Rev.Lett. 91, 262502 (2003).



(a) Fermi (b) Gamow-Teller transitions.
F. Osterfeld, Rev. Mod. Phys., 64, 491557 (1992).

Introduction and motivation: spin-isospin excitations

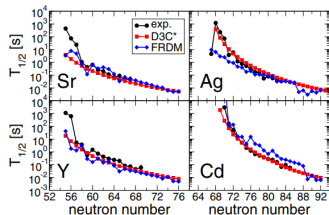
- ✓ ... and nuclear weak interaction processes in stellar environments:

- Calculation of the β -decay rates of r-process nuclei
J. Engel et al., Phys. Rev. C 60, 014302 (1999);
T. Marketin et al., Phys. Rev. C 93, 025805 (2015).
- Electron capture cross sections and rates
K. Langanke et al., Phys. Rev. Lett. 90, 241102 (2003);
A. L. Cole et al., Phys. Rev. C 86, 015809 (2012).
- and charged-current neutrino-nucleus reactions
N. Paar et al., Phys. Rev. C 77, 024608 (2008);
N. Paar et al., Phys. Rev. C 87, 025801 (2013).

... which take place at finite temperatures.

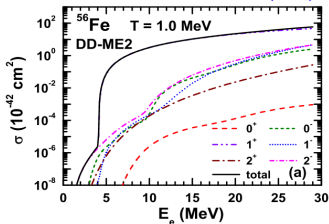
Therefore, accurate determination of the Gamow-Teller excitations as well as the nuclear properties is quite important for the astrophysical calculations.

Self-consistent mean-field theories (HF, QRPA) are standing as the prominent tools for calculations.



Beta decay half-lives.

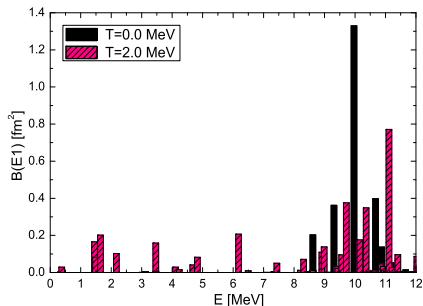
T. Marketin, et al., PRC 93, 025805 (2016).



Electron capture cross sections are calculated using FT-PNRPA.

Y.F. Niu et al., PRC 83, 045807 (2011).

Overview of recent works



The reduced transition probabilities for the low-energy dipole region at $T = 0$ MeV and $T = 2$ MeV.

- Derivation of the FT-QRPA equations:
H. M. Sommermann, *Ann. Phys. (NY)* **151**, 163 (1983).
- Finite temperature Continuum QRPA:
E. Khan et. al., *Nucl. Phys. A* **731**, 311 (2004).

TABLE II. The major low-energy dipole excitations for ^{68}Ni at $T = 0$ and 2 MeV. The configurations and their contribution to the norm of the states (in percentage) are displayed for each excitation energies, separately. The transitions appear by increasing the temperature are also shown in gray.

Configurations	$T = 0$ MeV	$T = 2$ MeV	$T = 2$ MeV
	E=10.05 MeV	E=9.62 MeV	E=11.0 MeV
$\nu 1f_{5/2} \rightarrow \nu 2d_{3/2}$	61.4	53.0	-
$\nu 1f_{7/2} \rightarrow \nu 1g_{9/2}$	9.7	4.6	9.4
$\nu 2p_{3/2} \rightarrow \nu 2d_{5/2}$	7.1	5.5	4.8
$\nu 1f_{5/2} \rightarrow \nu 2d_{5/2}$	5.0	2.4	-
$\nu 1f_{5/2} \rightarrow \nu 3d_{3/2}$	2.6	1.2	-
$\nu 1g_{9/2} \rightarrow \nu 2h_{11/2}$	-	2.6	18.7
$\nu 2d_{5/2} \rightarrow \nu 4f_{7/2}$	-	5.9	-
$\nu 2p_{3/2} \rightarrow \nu 3s_{1/2}$	-	-	4.8
$\pi 1f_{7/2} \rightarrow \pi 1g_{9/2}$	4.4	1.9	2.0
$\pi 1f_{5/2} \rightarrow \pi 2d_{5/2}$	-	10.1	-
$\pi 2p_{3/2} \rightarrow \pi 2d_{5/2}$	-	1.4	47.0
$\pi 1d_{5/2} \rightarrow \pi 1f_{7/2}$	-	-	3.5
$\pi 2s_{1/2} \rightarrow \pi 2p_{3/2}$	-	-	2.2

E. Yüksel, G. Colò, E. Khan, Y.F. Niu, K. Bozkurt *Phys. Rev. C* **96**, 024303 (2017).

Overview of recent works

Gamow-Teller transitions at finite temperature with the RPA:

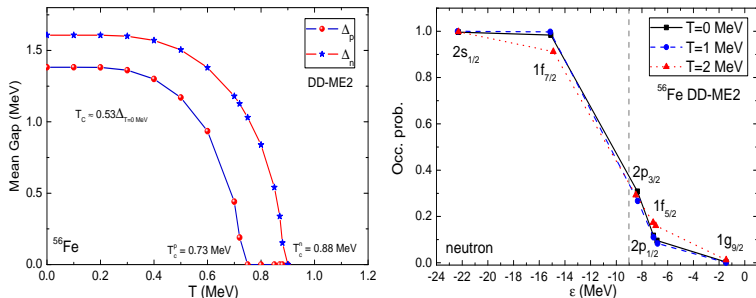
- ✓ The extended QRPA: O. Civitarese and M. Reboiro, *Phys. Rev. C* 63, 034323 (2001).
- ✓ Shell model+RPA: K. Langanke, E. Kolbe, and D. J. Dean, *Phys. Rev. C* 63, 032801(R) (2001).
- ✓ Thermo-Field-Dynamics (TFD) formalism: Alan A. Dzhihev et.al., *Phys. Rev. C* 81, 015804 (2010)
- ✓ Skyrme-TQRPA: Alan A. Dzhihev et.al., *Phys. Rev. C* 94, 015805 (2016).
- ✓ FT-RRPA: Y.F. Niu et.al., *Phys. Rev. C* 83, 045807 (2011).

Goal

- There is no complete investigation available on the effect of the temperature on the spin-isospin response of the open-shell nuclei using relativistic nuclear energy density functionals!
- The purpose of the present work is to investigate the finite temperature effects on the Gamow-Teller excitations by developing the self consistent relativistic finite temperature proton-neutron QRPA.

Finite temperature effects on the ground state properties

The relativistic nuclear energy density functional with density dependent meson-nucleon couplings are used in the calculations, and pairing correlations are taken into account in the BCS scheme.



Left: Mean value of the neutron(proton) pairing gap as a function of the temperature for ^{56}Fe . Right: occupation probabilities for neutron states as a function of temperature. The calculations are performed using DD-ME2 functional.

Temperature dependent Fermi-Dirac distribution function: $f_i = [1 + \exp(E_i/k_B T)]^{-1}$

Microscopic model: Finite temperature quasiparticle random phase approximation

The starting point in the Equation of Motion (EOM) method is the definition of a suitable excitation operator

$$\Gamma_{\nu}^{\dagger} = \sum_{a \geq b} X_{ab}^{\nu} a_a^{\dagger} a_b^{\dagger} - Y_{ab}^{\nu} a_b a_a + P_{ab}^{\nu} a_a^{\dagger} a_b - Q_{ab}^{\nu} a_b^{\dagger} a_a \quad (1)$$

two-quasiparticle creation/destruction operators and one-quasiparticle creation/ destruction operators. With $|BCS\rangle$ as the approximate thermal vacuum the equation of motion can be written as:

$$\langle BCS | [\delta\Gamma, H, \Gamma_{\nu}^{\dagger}] | BCS \rangle = E_{\nu} \langle BCS | [\delta\Gamma, \Gamma_{\nu}^{\dagger}] | BCS \rangle \quad (2)$$

The FT-QRPA equations are derived as:

$$\tilde{A}_{abcd} = \sqrt{1 - f_a - f_b} A'_{abcd} \sqrt{1 - f_c - f_d} + (E_a + E_b) \delta_{ac} \delta_{bd}, \quad (3)$$

$$\tilde{B}_{abcd} = \sqrt{1 - f_a - f_b} B_{abcd} \sqrt{1 - f_c - f_d}, \quad (4)$$

$$\tilde{C}_{abcd} = \sqrt{f_b - f_a} C'_{abcd} \sqrt{f_d - f_c} + (E_a - E_b) \delta_{ac} \delta_{bd}, \quad (5)$$

$$\tilde{D}_{abcd} = \sqrt{f_b - f_a} D_{abcd} \sqrt{f_d - f_c}, \quad (6)$$

$$\tilde{a}_{abcd} = \sqrt{f_b - f_a} a_{abcd} \sqrt{1 - f_c - f_d}, \quad (7)$$

$$\tilde{b}_{abcd} = \sqrt{f_b - f_a} b_{abcd} \sqrt{1 - f_c - f_d}, \quad (8)$$

H. M. Sommermann, Ann. Phys. (NY) 151, 163 (1983).

E. Yüksel, G. Colò, E. Khan, Y.F. Niu, K. Bozkurt Phys. Rev. C. 96, 024303 (2017).

Microscopic model: finite temperature quasiparticle random phase approximation

The matrix elements read:

$$\begin{aligned} A'_{abcd} = & (u_a u_b u_c u_d + v_a v_b v_c v_d) V_{abcd} \\ & + (u_a v_b u_c v_d + v_a u_b v_c u_d) V_{a\bar{d}\bar{b}c} \\ & - (-1)^{j_c+j_d+J} (u_a v_b v_c u_d + v_a u_b u_c v_d) V_{a\bar{c}\bar{b}d} \end{aligned} \quad (9)$$

$$\begin{aligned} B_{abcd} = & -(u_a u_b v_c v_d + v_a v_b u_c u_d) V_{ab\bar{c}\bar{d}} \\ & + (u_a v_b v_c u_d + v_a u_b u_c v_d) V_{ad\bar{c}\bar{b}} \\ & - (-1)^{j_c+j_d+J} (u_a v_b u_c v_d + v_a u_b v_c u_d) V_{ac\bar{b}\bar{d}} \end{aligned} \quad (10)$$

$$\begin{aligned} C'_{abcd} = & (u_a v_b u_c v_d + v_a u_b v_c u_d) V_{a\bar{b}\bar{c}\bar{d}} \\ & + (u_a u_b u_c u_d + v_a v_b v_c v_d) V_{adbc} \\ & + (-1)^{j_c+j_d+J} (u_a u_b v_c v_d + v_a v_b u_c u_d) V_{a\bar{c}\bar{b}\bar{d}} \end{aligned} \quad (11)$$

$$\begin{aligned} D_{abcd} = & (u_a v_b v_c u_d + v_a u_b u_c v_d) V_{a\bar{b}\bar{c}\bar{d}} \\ & - (u_a u_b v_c v_d + v_a v_b u_c u_d) V_{a\bar{d}\bar{b}\bar{c}} \\ & - (-1)^{j_c+j_d+J} (u_a u_b u_c u_d + v_a v_b v_c v_d) V_{acbd} \end{aligned} \quad (12)$$

Microscopic model: finite temperature quasiparticle random phase approximation

$$\begin{aligned}
 a_{abcd} = & (v_a u_b v_c v_d - u_a v_b u_c u_d) V_{\bar{a}bcd}^{pp} \\
 & - (v_a v_b v_c u_d - u_a u_b u_c v_d) V_{\bar{a}\bar{d}bc}^{ph} \\
 & + (-1)^{j_c + j_d + J} (v_a v_b u_c v_d - u_a u_b v_c u_d) V_{\bar{a}\bar{c}bd}^{ph}
 \end{aligned} \tag{13}$$

$$\begin{aligned}
 b_{abcd} = & - (v_a u_b u_c u_d - u_a v_b v_c v_d) V_{\bar{a}bcd}^{pp} \\
 & - (v_a v_b u_c v_d - u_a u_b v_c u_d) V_{\bar{a}db\bar{c}}^{ph} \\
 & + (-1)^{j_c + j_d + J} (v_a v_b v_c u_d - u_a u_b u_c v_d) V_{\bar{a}cb\bar{d}}^{ph}
 \end{aligned} \tag{14}$$

$$\begin{aligned}
 a_{abcd}^+ = & (v_a v_b v_c u_d - u_a u_b u_c v_d) V_{\bar{a}bc\bar{d}}^{pp} \\
 & - (v_a u_b v_c v_d - u_a v_b u_c u_d) V_{\bar{a}\bar{d}\bar{b}c}^{ph} \\
 & - (-1)^{j_c + j_d + J} (v_a u_b u_c u_d - u_a v_b v_c v_d) V_{\bar{a}\bar{c}bd}^{ph}
 \end{aligned} \tag{15}$$

$$\begin{aligned}
 b_{abcd}^T = & (v_a v_b u_c v_d - u_a u_b v_c u_d) V_{\bar{a}b\bar{c}\bar{d}}^{pp} \\
 & + (v_a u_b u_c u_d - u_a v_b v_c v_d) V_{\bar{a}\bar{d}bc}^{ph} \\
 & + (-1)^{j_c + j_d + J} (v_a u_b v_c v_d - u_a v_b u_c u_d) V_{\bar{a}c\bar{b}\bar{d}}^{ph}
 \end{aligned} \tag{16}$$

Microscopic model: Finite temperature quasiparticle random phase approximation

The finite temperature QRPA equations can be combined into a single matrix as

$$\begin{pmatrix} \tilde{C} & \tilde{a} & \tilde{b} & \tilde{D} \\ \tilde{a}^+ & \tilde{A} & \tilde{B} & \tilde{b}^T \\ -\tilde{b}^+ & -\tilde{B}^* & -\tilde{A}^* & -\tilde{a}^T \\ -\tilde{D}^* & -\tilde{b}^* & -\tilde{a}^* & -\tilde{C}^* \end{pmatrix} \begin{pmatrix} \tilde{P} \\ \tilde{X} \\ \tilde{Y} \\ \tilde{Q} \end{pmatrix} = \hbar\omega \begin{pmatrix} \tilde{P} \\ \tilde{X} \\ \tilde{Y} \\ \tilde{Q} \end{pmatrix} \quad (17)$$

- \tilde{A} and \tilde{B} (and their complex conjugates) describe the effects of two-quasiparticle excitations ($a^\dagger a^\dagger$ and aa).

$$\sum_{a \geq b} \left\{ |\tilde{X}_{ab}^\nu|^2 - |\tilde{Y}_{ab}^\nu|^2 + |\tilde{P}_{ab}^\nu|^2 - |\tilde{Q}_{ab}^\nu|^2 \right\} = 1, \quad (18)$$

The reduced transition probability is given as

$$B(EJ, \tilde{0} \rightarrow \nu) = |\langle \nu || \hat{F}_J || \tilde{0} \rangle|^2 \\ = \left| \sum_{c \geq d} \left\{ (\tilde{X}_{cd}^\nu + \tilde{Y}_{cd}^\nu)(v_c u_d + u_c v_d) \sqrt{1 - f_c - f_d} + (\tilde{P}_{cd}^\nu + \tilde{Q}_{cd}^\nu)(u_c u_d - v_c v_d) \sqrt{f_d - f_c} \right\} \langle c || \hat{F}_J || d \rangle \right|^2. \quad (19)$$

Numerical results - finite temperature effects

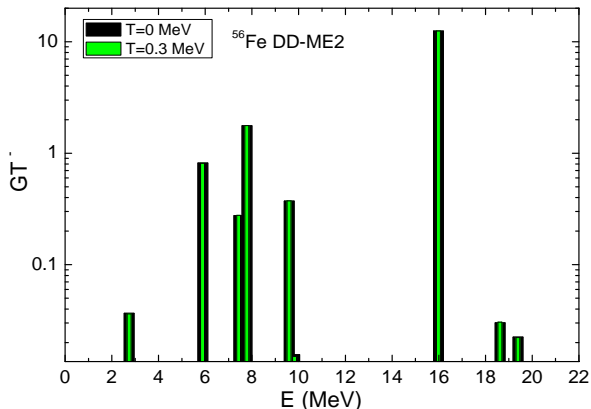


Figure 2: The Gamow-Teller strength in ^{56}Fe by increasing temperature. The FT-PNQRPA calculations are performed on top of the FT-HBCS. The strength of the $T = 0$ particle-particle interaction is taken as $V_0 = 200\text{MeV}$.

- The main GT^- strength at $E=15.98$ MeV is formed with $\nu 1f_{7/2} \rightarrow \pi 1f_{5/2}$ transition.
- By increasing the temperature, at $T=0.3$ MeV, Gamow-Teller strength and excitation energies do not change.

Numerical results - finite temperature effects

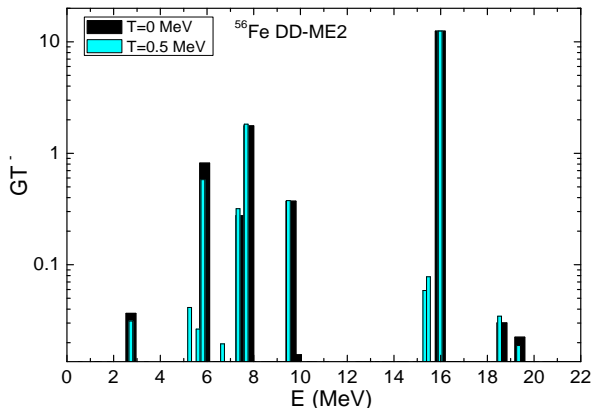


Figure 3: The Gamow-Teller strength in ^{56}Fe by increasing temperature.

- At $T=0.5$ MeV, the main Gamow-Teller strength and excitation energy do not change.
- Formation of the new Gamow-Teller states is obtained due to the changes in the occupation probabilities of states and opening of the new excitation channels.

Numerical results - finite temperature effects

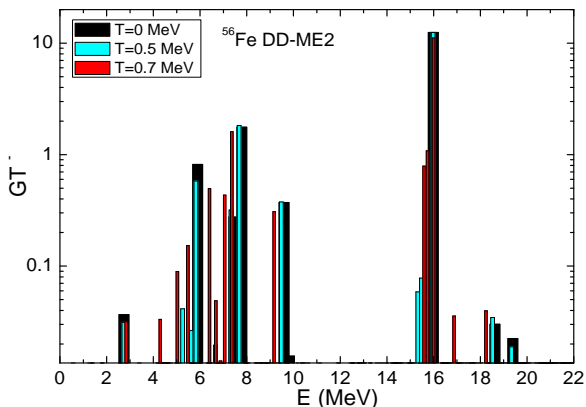


Figure 4: The Gamow-Teller strength in ^{56}Fe by increasing temperature.

- Increasing the temperature further, the main peak at around 16 MeV is almost not affected, whereas the Gamow-Teller states shift toward downward in the low-energy region.
- With the formation of the new states, the low-energy region becomes more fragmented.
- Ikeda Sum rule is satisfied at finite temperature.

Numerical results - finite temperature effects

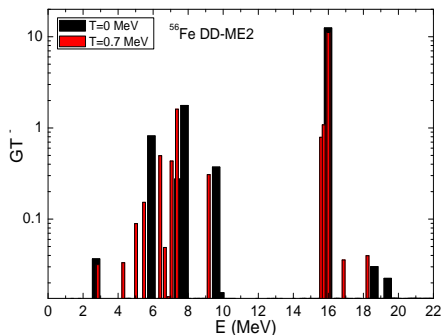


Figure 5: The Gamow-Teller (GT^-) strength in ^{56}Fe using DD-ME2 interaction.

Table: the selected low-energy states and corresponding transitions at $T=0.7$ MeV.

E (MeV)	Transitions
4.30	$\nu 2p_{1/2} \rightarrow \pi 2p_{3/2}$ (99.64%)
5.48	$\nu 2p_{3/2} \rightarrow \pi 2p_{3/2}$ (98.26%)
6.40	$\nu 1f_{7/2} \rightarrow \pi 1f_{7/2}$ (91.7%)
	$\nu 2p_{3/2} \rightarrow \pi 2p_{3/2}$ (2.44%)
7.05	$\nu 1f_{5/2} \rightarrow \pi 2p_{3/2}$ (50.47%)
	$\nu 2p_{3/2} \rightarrow \pi 1f_{5/2}$ (12.64%)
	$\nu 2p_{3/2} \rightarrow \pi 2p_{1/2}$ (14.10%)
7.35	$\nu 2p_{3/2} \rightarrow \pi 2p_{3/2}$ (49.95%)
	$\nu 2p_{1/2} \rightarrow \pi 2p_{3/2}$ (20.58%)
	$\nu 1f_{5/2} \rightarrow \pi 2p_{3/2}$ (12.92%)

- Apart from $(E_a + E_b)$ configurations, $(E_a - E_b)$ two q.p. configurations also start to contribute to the excitations. This mainly affects the low-energy region with increasing temperature.

Numerical results - temperature.vs.isovector pairing effects

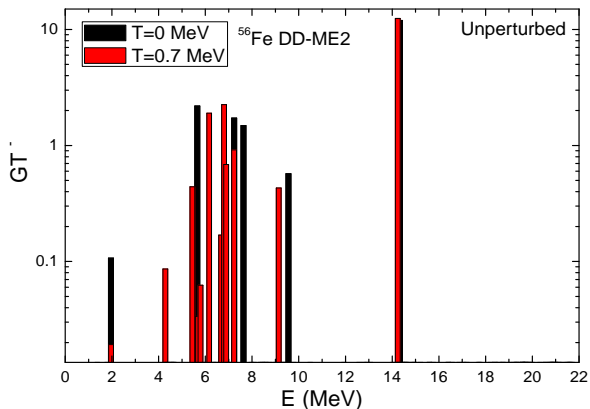


Figure 6: Unperturbed GT^- strength at $T=0$ and 0.7 MeV.

- Isovector pairing ($T=1$) \downarrow and E_{conf} \downarrow .

Numerical results - temperature vs. isoscalar pairing effects

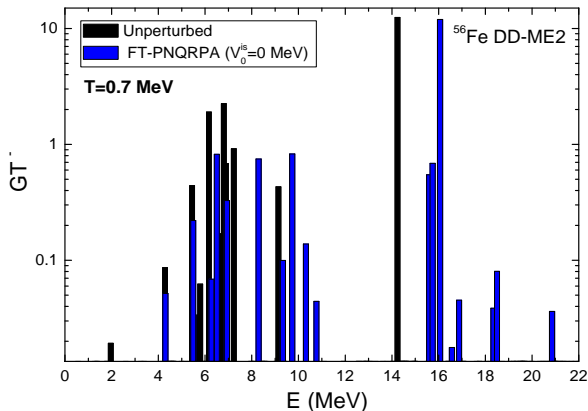


Figure 7: Unperturbed and FT-PNQRPA results for the GT^- strength at $T=0$ and 0.7 MeV.

$$V_{12} = -V_0 \sum_{j=1}^2 g_j e^{-r_{12}^2/\mu_j^2} \hat{\Pi}_{S=1, T=0}$$

- ...where $\mu_1 = 1.2\text{fm}$, $\mu_2 = 0.7\text{fm}$ and $g_1 = 1$, $g_2 = -2$. Here, V_0 is a free parameter.

Numerical results - temperature vs. isoscalar pairing effects

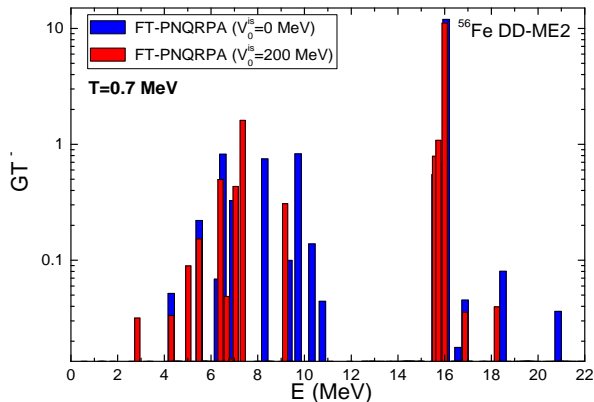


Figure 8: Unperturbed and FT-PNQRPA results for the GT^- strength at $T=0$ and 0.7 MeV.

$$V_{12} = -V_0 \sum_{j=1}^2 g_j e^{-t_{12}^2/\mu_j^2} \hat{\Pi}_{S=1, T=0}$$

- The isoscalar pairing shifts the excitation energies down and the strength is enhanced in the low-energy region.

Numerical results - FT-PNRPA vs. FT-PNQRPA

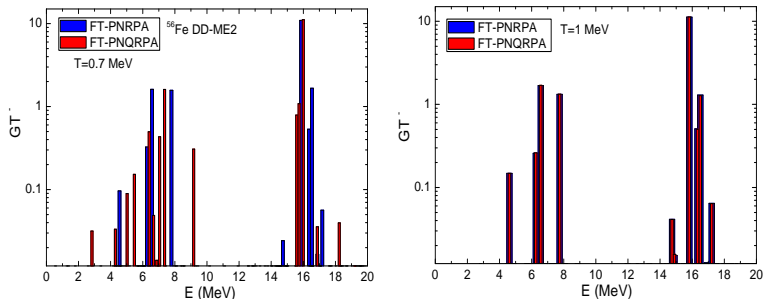


Figure 7: Comparison of the Gamow-Teller strength in ^{56}Fe using FT-PNRPA and FT-PNQRPA.

- Inclusion of the pairing in microscopic models is important for the proper description of the Gamow-Teller states below the critical temperatures.

Conclusions

The relativistic finite temperature proton-neutron QRPA is developed and used in the calculations of the Gamow-Teller response of nuclei.

- For $T \geq 0.5$ MeV, formation of the new low-energy strengths are obtained with the opening of the new excitation channels.
- The Gamow-Teller excitation energies also start to shift downward by increasing temperature.
- Inclusion of the pairing in microscopic models is crucial for the proper description of the Gamow-Teller states below the critical temperatures.

Perspectives

- The other spin-isospin resonances in nuclei at Finite Temperature?
- Calculation of the nuclear weak interaction processes (beta decay, electron capture, neutrino-nucleus scattering etc.,) at finite temperature.

Acknowledgments



Collaborators

Nils Paar (University of Zagreb, Croatia)

Gianluca Colò (Università degli Studi di Milano and INFN)

Elias Khan (Institut de Physique Nucléaire, Université Paris-Sud)

Yifei Niu (INFN, ELI-NP)

Funding

This work was supported by the QuantiXLie Centre of Excellence, a project co-financed by the Croatian Government and European Union through the European Regional Development Fund - the Competitiveness and Cohesion Operational Program (Grant KK.01.1.1.01.0004).

For more information please visit:
<http://bela.phy.hr/quantixlie/hr/>
<https://strukturnifondovi.hr/>

The sole responsibility for the content of this presentation lies with the Faculty of Science, University of Zagreb. It does not necessarily reflect the opinion of the European Union.



Europska unija
Zajedno do fondova EU



EUROPSKI STRUKTURNI
I INVESTICIJSKI FONDovi



Operativni program
**KONKURENTNOST
I KOHEZIJA**

Co-financed by the European Union through the European Regional Development Fund

The quasiparticle representation of the Hamiltonian

The Hamiltonian is defined in particle basis as:

$$H = \sum_{ab} T_{ab} c_a^\dagger c_b + \frac{1}{4} \sum_{abcd} v_{abcd} c_a^\dagger c_b^\dagger c_d c_c \quad (20)$$

here, T represents the kinetic energy and the v_{abcd} are antisymmetrized matrix elements of the nuclear interaction. The transformation from particles to quasiparticles is performed through

$$c_a^\dagger = u_a \tilde{a}_a^\dagger - v_a \tilde{a}_a, \tilde{c}_a = u_a a_a - v_a \tilde{a}_a^\dagger \quad (21)$$

and we obtain the Hamiltonian as

$$H = H_0 + \sum_b H_{11}(b) [a_b^\dagger \tilde{a}_b] + \sum_b H_{20}(b) ([a_b^\dagger \tilde{a}_b] - [\tilde{a}_b a_b]) + V_{RES} \quad (22)$$

The residual interaction is given in compact form as

$$V_{RES} = \frac{1}{4} \sum_{abcd} \bar{v}_{abcd} N [c_a^\dagger c_b^\dagger c_d c_c] \quad (23)$$

where $N[\dots]$ BCS denotes normal ordering with respect to the BCS vacuum ($|BCS\rangle$). Expressing the residual interaction in terms of the quasiparticle creation and annihilation operators, V_{RES} is written as

$$V_{RES} = H_{40} + H_{31} + H_{22} \quad (24)$$

$$H_{40} = \sum_{abcd} \bar{v}_{abcd} \left[\frac{1}{4} u_a u_b v_c v_d (: a_a^\dagger a_b^\dagger \tilde{a}_d^\dagger \tilde{a}_c^\dagger : + H.c.) \right] \quad (25)$$

$$H_{31} = \sum_{abcd} \bar{v}_{abcd} \left[-\frac{1}{2} (u_a u_b u_c v_d - v_a v_b v_c u_d) (: a_a^\dagger a_b^\dagger \tilde{a}_d^\dagger a_c : + H.c.) \right] \quad (26)$$

$$H_{22} = \sum_{abcd} \bar{v}_{abcd} \left[\frac{1}{4} (u_a u_b u_c u_d + v_a v_b v_c v_d) (: a_a^\dagger a_b^\dagger a_d a_c : - u_a v_b u_c v_d : a_a^\dagger \tilde{a}_d^\dagger \tilde{a}_b a_c : \right] \quad (27)$$

Microscopic model: finite temperature quasiparticle random phase approximation

The starting point in the Equation of Motion (EOM) method is the definition of a suitable excitation operator

$$\Gamma_{\nu}^{\dagger} = \sum_{a \geq b} X_{ab}^{\nu} A_{ab}^{\dagger}(JM) - Y_{ab}^{\nu} A_{ab}(\widetilde{JM}) + P_{ab}^{\nu} B_{ab}^{\dagger}(JM) - Q_{ab}^{\nu} B_{ab}(\widetilde{JM}) \quad (28)$$

here $\nu = nJ^{\pi}M$ and the summation is restricted to avoid double counting. The Hermitian of Γ_{ν}^{\dagger} is:

$$\Gamma_{\nu} = \sum_{a \geq b} X_{ab}^{\nu*} A_{ab}(JM) - Y_{ab}^{\nu*} A_{ab}^{\dagger}(\widetilde{JM}) + P_{ab}^{\nu*} B_{ab}(JM) - Q_{ab}^{\nu*} B_{ab}^{\dagger}(\widetilde{JM}). \quad (29)$$

We define the coupled operators as:

$$A_{ab}^{\dagger}(JM) = N_{ab}(J) \sum_{m_a m_b} \langle j_a m_a j_b m_b | JM \rangle a_a^{\dagger} a_b^{\dagger}, \quad (30)$$

$$A_{ab}(\widetilde{JM}) = N_{ab}(J) (-)^{J+M} \sum_{m_a m_b} \langle j_a m_a j_b m_b | J - M \rangle a_b a_a, \quad (31)$$

$$B_{ab}^{\dagger}(JM) = N_{ab}(J) \sum_{m_a m_b} (-)^{j_b - m_b} \langle j_a m_a j_b - m_b | JM \rangle a_a^{\dagger} a_b, \quad (32)$$

$$B_{ab}(\widetilde{JM}) = N_{ab}(J) (-)^{J+M} \sum_{m_a m_b} (-)^{j_b - m_b} \langle j_a m_a j_b - m_b | J - M \rangle a_b^{\dagger} a_a. \quad (33)$$

where a^{\dagger} and a are the quasiparticle operators and N_{ab} is defined as

$$N_{ab}(J) = \frac{\sqrt{1 + (-)^J \delta_{ab}}}{1 + \delta_{ab}}. \quad (34)$$

Basic variations can be written as

$$\delta\Gamma = A_{ab}(JM)(B_{ab}(JM)), \quad \delta\Gamma = A_{ab}^{\dagger}(\widetilde{JM})(B_{ab}^{\dagger}(\widetilde{JM})) \quad (35)$$

Microscopic model: finite temperature quasiparticle random phase approximation

The matrix elements read:

$$\begin{aligned} A'_{abcd} &= (u_a u_b u_c u_d + v_a v_b v_c v_d) V_{abcd} \\ &+ N_{ab}(J) N_{cd}(J) [(u_a v_b u_c v_d + v_a u_b v_c u_d) V_{a\bar{d}\bar{b}c} \\ &- (-1)^{j_c + j_d + J} (u_a v_b v_c u_d + v_a u_b u_c v_d) V_{a\bar{c}\bar{b}d}] \end{aligned} \quad (36)$$

$$\begin{aligned} B_{abcd} &= -(u_a u_b v_c v_d + v_a v_b u_c u_d) V_{ab\bar{c}\bar{d}} \\ &+ N_{ab}(J) N_{cd}(J) [(u_a v_b v_c u_d + v_a u_b u_c v_d) V_{ad\bar{c}\bar{b}} \\ &- (-1)^{j_c + j_d + J} (u_a v_b u_c v_d + v_a u_b v_c u_d) V_{ac\bar{b}\bar{d}}] \end{aligned} \quad (37)$$

$$\begin{aligned} C'_{abcd} &= (u_a v_b u_c v_d + v_a u_b v_c u_d) V_{a\bar{b}\bar{c}\bar{d}} \\ &+ N_{ab}(J) N_{cd}(J) [(u_a u_b u_c u_d + v_a v_b v_c v_d) V_{adbc} \\ &+ (-1)^{j_c + j_d + J} (u_a u_b v_c v_d + v_a v_b u_c u_d) V_{a\bar{c}\bar{b}d}] \end{aligned} \quad (38)$$

$$\begin{aligned} D_{abcd} &= (u_a v_b v_c u_d + v_a u_b u_c v_d) V_{a\bar{b}\bar{c}d} \\ &- N_{ab}(J) N_{cd}(J) [(u_a u_b v_c v_d + v_a v_b u_c u_d) V_{a\bar{d}\bar{b}c} \\ &+ (-1)^{j_c + j_d + J} (u_a u_b u_c u_d + v_a v_b v_c v_d) V_{acbd}] \end{aligned} \quad (39)$$

Microscopic model: finite temperature quasiparticle random phase approximation

$$\begin{aligned}
 a_{abcd} = & (v_a u_b v_c v_d - u_a v_b u_c u_d) V_{a\bar{b}cd}^{pp} \\
 & - N_{ab}(J) N_{cd}(J) [(v_a v_b v_c v_d - u_a u_b u_c v_d) V_{a\bar{d}bc}^{ph} \\
 & - (-1)^{j_c + j_d + J} (v_a v_b u_c v_d - u_a u_b v_c u_d) V_{a\bar{c}bd}^{ph}]
 \end{aligned} \tag{40}$$

$$\begin{aligned}
 b_{abcd} = & - (v_a u_b u_c u_d - u_a v_b v_c v_d) V_{\bar{a}bcd}^{pp} \\
 & - N_{ab}(J) N_{cd}(J) [(v_a v_b u_c v_d - u_a u_b v_c u_d) V_{\bar{a}db\bar{c}}^{ph} \\
 & - (-1)^{j_c + j_d + J} (v_a v_b v_c u_d - u_a u_b u_c v_d) V_{\bar{a}cb\bar{d}}^{ph}]
 \end{aligned} \tag{41}$$

$$\begin{aligned}
 a_{abcd}^+ = & (v_a v_b v_c u_d - u_a u_b u_c v_d) V_{abc\bar{d}}^{pp} \\
 & - N_{ab}(J) N_{cd}(J) [(v_a u_b v_c v_d - u_a v_b u_c u_d) V_{ad\bar{b}c}^{ph} \\
 & + (-1)^{j_c + j_d + J} (v_a u_b u_c u_d - u_a v_b v_c v_d) V_{\bar{a}cb\bar{d}}^{ph}]
 \end{aligned} \tag{42}$$

$$\begin{aligned}
 b_{abcd}^T = & (v_a v_b u_c v_d - u_a u_b v_c u_d) V_{ab\bar{c}d}^{pp} \\
 & + N_{ab}(J) N_{cd}(J) [(v_a u_b u_c u_d - u_a v_b v_c v_d) V_{\bar{a}db\bar{c}}^{ph} \\
 & + (-1)^{j_c + j_d + J} (v_a u_b v_c v_d - u_a v_b u_c u_d) V_{\bar{a}c\bar{b}d}^{ph}]
 \end{aligned} \tag{43}$$